International Journal of Mechanical Sciences 131–132 (2017) 938–955

Contents lists available at ScienceDirect

International Journal of Mechanical Sciences

journal homepage: www.elsevier.com/locate/ijmecsci

Damage evolution of fiber-reinforced ceramic-matrix composites under stress-rupture and cyclic loading at elevated temperature in oxidizing atmosphere

Li Longbiao

College of Civil Aviation, Nanjing University of Aeronautics and Astronautics, No. 29 Yudao St., Nanjing 210016, PR China

ARTICLE INFO

Keywords:
Ceramic-matrix composites (CMCs)
Damage evolution
Oxidation
Matrix cracking
Interface debonding

ABSTRACT

In this paper, the damage evolution of fiber-reinforced ceramic-matrix composites (CMCs) subjected to stress-rupture and cyclic fatigue loading at elevated temperatures in oxidizing atmospheres has been investigated. The damage parameters of hysteresis dissipated energy, hysteresis modulus, peak strain and hysteresis width have been used to monitor the damage evolution inside of CMCs. The effects of the hold time, stress levels, matrix crack spacing, fiber volume fraction and oxidation temperature on the evolution of damage parameters versus applied cycles have been analyzed. The experimental fatigue hysteresis loops, interface slip lengths, fatigue hysteresis dissipated energy and peak strain of cross-ply SiC/MAS, 2D SiC/SiC and Nextel™ 720/Alumina composites subjected to cyclic fatigue and stress-rupture at elevated temperatures have been predicted.

1. Introduction

Ceramic materials possess high strength and modulus at elevated temperature. But their use as structural components is severely limited because of their brittleness. Continuous fiber-reinforced ceramic-matrix composites, by incorporating fibers in ceramic matrices, however, not only exploit their attractive high-temperature strength but also reduce the propensity for catastrophic failure [1–3]. The critical nature of the application of these advanced materials makes complete characterization a necessary. The designers must have information pertaining to not only the strength of the material, but also its fatigue and toughness characteristics. Since CMCs have applications typically in the aerospace industry, these characteristics are especially important due to the severe operating environments encountered and lower safety factors imposed by weight considerations. Typically, the tests performed are monotonic loading, cyclic fatigue, and stress rupture at a variety of temperatures and/or atmosphere conditions. Most of the tests are conducted independently. However, these do not accurately represent the loading conditions encountered by an aircraft component. For example, a wing spar will encounter stress rupture type loading through the flight due to the weight of the airframe it is supporting. It will also encounter cyclic fatigue loading due to the mechanical vibrations from the engines and aerodynamic forces. The temperature will change dramatically with changes in altitude and flight Mach number. But the airframe as a whole will not suffer any of these stresses independently, there will always be some combination of these stresses acting on it at any time. It is possible that the cumulative damage caused to a component under a period of service is some combination of mechanisms caused by the cyclic fatigue, stress rupture and environment (i.e., temperature).

Many researchers performed the experimental and theoretical investigations on the stress-rupture and cyclic fatigue behavior of fiber-reinforced CMCs. Lara–Curzio [4] developed a micromechanical model to predict the reliability and lifetime of unidirectional CMCs subjected to stresses beyond the first matrix cracking stress at elevated temperature. It was shown that the oxidation of the fiber coating leads to changes in the stress distribution of fibers and exposure of the fibers to the environment, and the oxidation of the fibers leads to fiber strength degradation and ultimately composite fracture. Halverson and Curtin [5] investigated the deformation, strength and stress-rupture lifetime of an oxide/oxide CMC at temperatures of 950 °C and 1050 °C without considering oxidative attack, using a stress-rupture model incorporating the fiber strength statistics, fiber degradation with time and load, the matrix damage, and the fiber pullout with the Global Load Sharing (GLS) criterion. Sullivan [6] investigated the stress-rupture strength of SiC/SiC composite with a boron nitride (BN) fiber coating at the intermediate temperature range of 700–950 °C. It was found that the stress rupture strength of the composite decreases with increasing time, attributed almost entirely to the slow flaw growth within the fibers. Ruggles–Wrenn et al. [7] investigated the tension-tension fatigue behavior of 2D SiC/SiC composite at 1200 °C in air and in steam environments. The fatigue limit and fatigue lifetime decreases with increasing of the loading frequency from 0.1 to 10 Hz in both test environments, and the presence of

E-mail address: llb451@nuaa.edu.cn

http://dx.doi.org/10.1016/j.ijmecsci.2017.08.009
Received 5 January 2017; Received in revised form 10 July 2017; Accepted 5 August 2017
Available online 12 August 2017
0020-7403/

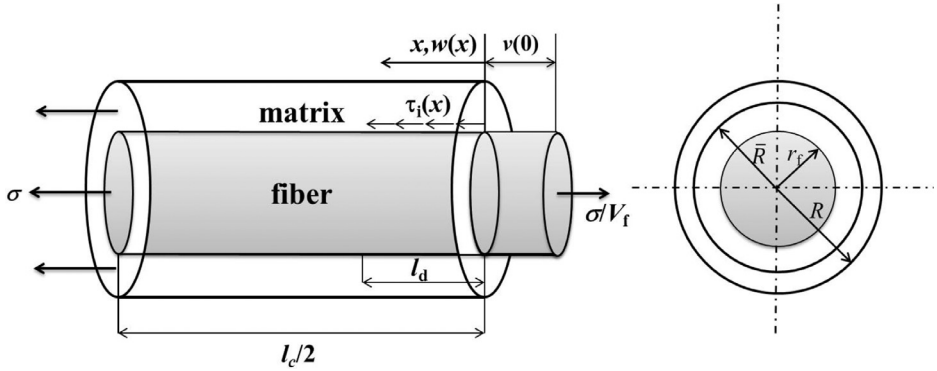

Fig. 1. The unit cell of Budiansky–Hutchinson–Evans shear-lag model.

steam significantly degraded the fatigue performance. Ruggles-Wrenn and Lanser [8] investigated the tension–compression fatigue behavior of 2D Nextel^{TM} 720/Alumina composite at 1200 ˚C in air and in steam atmospheres. The fatigue limit stress was achieved at 40% and 35% tensile strength in air and steam environment, respectively, when the maximum cycle number is defined to be 100,000 applied cycles. The presence of steam noticeably degrades the tension–compression fatigue performance of the oxide/oxide composite. Ruggles-Wrenn and Lee [9] investigated the tension−tension fatigue behavior of 2D SiC/SiC composite with an inhibited matrix at 1300 ˚C in air and in steam conditions. The fatigue limit stress is higher in steam environment than that in air, which indicates that the presence of steam appears to have a moderately beneficial effect on the tension-tension fatigue at 1300 ˚C. Under stress rupture and cyclic loading, the damage evolution inside the composites should be monitored to predict the lifetime of CMCs. Maillet et al. [10] investigated the damage evolution in 2D SiC/[Si−B−C] composite at temperatures of 450 ˚C and 500 ˚C using the Acoustic Emission (AE) based approach under static fatigue loading. However, the AE based approach used to damage monitoring is limited at elevated temperature. Li [11,12] developed a hysteresis dissipated energy-based damage parameter for damage evolution and life prediction of fiber-reinforced CMCs under cyclic fatigue loading at room and elevated temperatures.

The objective of this paper is to investigate the damage evolution of fiber-reinforced CMCs under stress-rupture and cyclic loading at elevated temperatures. The Budiansky–Hutchinson–Evans shear-lag model was used to describe the micro stress field of the damaged composite considering interface wear and interface oxidation. The statistical matrix multicracking model and fracture mechanics interface debonding criterion were used to determine the matrix crack spacing and interface debonded length. The damage parameters of the fatigue hysteresis dissipated energy, hysteresis modulus, peak strain and hysteresis width have been used to monitor the damage evolution inside of CMCs. The effects of the hold time, stress level, matrix crack spacing, fiber volume content and oxidation temperature on the evolution of damage parameters verus cycle numbers have been investigated. The experimental fatigue hysteresis loops, the interface slip lengths, fatigue hysteresis dissipated energy, and the peak strain of cross-ply SiC/MAS, 2D SiC/SiC and Nextel^{TM} 720/Alumina composites under cyclic fatigue and stress-rupture at elevated temperatures have been predicted.

2. Stress analysis

When the applied stress σ is higher than the matrix cracking stress, matrix multicracking and interface debonding occur. The unit cell contained a single fiber surrounded by a hollow cylinder of matrix is extracted from the ceramic composite system, as shown in Fig. 1. The fiber radius is r_f, and the matrix radius is R ($R = r_f/V_f^{1/2}$). The length of the unit cell is half of the matrix crack spacing $l_c/2$. Budiansky et al. [13] assumed that the matrix axial load is concentrated at $\overline{R}$ and the region between r_f and $\overline{R}$ only carries the shear stress. At elevated temperature, matrix cracks will serve as avenues for the ingress of the environment atmosphere into composite, as shown in Fig. 2. The oxygen reacts with the interphase layer along the fiber length at a certain rate of $d\xi/dt$, in which ξ is the length of interphase lost in each side of the crack [14].

$$\xi = \varphi_1\left[1-\exp\left(-\frac{\varphi_2 t}{b}\right)\right] \tag{1}$$

where φ_1 and φ_2 are parameters dependent on temperature and described using the Arrhenius type laws [14].

Under cyclic loading, the interface shear stress decreases due to the interface wear. The interface debonded region can be divided into two regions, including:

(1) The interface oxidation region, i.e., $x\in[0, \xi]$, the stress transfer between the fiber and the matrix is controlled by a sliding stress $\tau_i(x)=\tau_f$.
(2) The interface wear region, i.e., $x\in[\xi, l_d]$, the stress transfer between the fiber and the matrix is controlled by a sliding stress $\tau_i(x)=\tau_i(N)$, in which $\tau_i(N)$ denotes the interface shear stress at the Nth applied cycle. [15]

$$\left(\tau_i(N)-\tau_s\right)/\left(\tau_0-\tau_s\right) = \left(1+b_0\right)\left(1+b_0N^j\right)^{-1} \tag{2}$$

where τ_0 denotes the initial interface shear stress; τ_s denotes the steady-state interface shear stress; b_0 is a coefficient; and j is an exponent which determines the rate at which interface shear stress drops with the number of cycle N.

The axial stress distributions of the fiber, matrix and the interface shear stress in the interface oxidation region ($x\in[0, \xi]$), the interface wear region ($x\in[\xi, l_d]$) and the interface bonded region ($x\in[l_d, l_c/2]$) are given by Eq. (3).

$$\sigma_f(x)=\begin{cases}\dfrac{\sigma}{V_f}-\dfrac{2\tau_f}{r_f}x, x\in(0,\xi)\\ \dfrac{\sigma}{V_f}-\dfrac{2\tau_f}{r_f}\xi-\dfrac{2\tau_i(N)}{r_f}(x-\xi), x\in(\xi,l_d)\\ \sigma_{fo}+\left[\dfrac{V_m}{V_f}\sigma_{mo}-2\dfrac{\tau_f}{r_f}\xi-2\dfrac{\tau_i(N)}{r_f}(l_d-\xi)\right]\\ \quad\exp\left(-\rho\dfrac{x-l_d}{r_f}\right), x\in\left(l_d,\dfrac{l_c}{2}\right)\end{cases} \tag{3a}$$

$$\sigma_m(x)=\begin{cases}2\dfrac{V_f}{V_m}\dfrac{\tau_f}{r_f}x, x\in(0,\xi)\\ 2\dfrac{V_f}{V_m}\dfrac{\tau_f}{r_f}\xi+2\dfrac{V_f}{V_m}\dfrac{\tau_i(N)}{r_f}(x-\xi), x\in(\xi,l_d)\\ \sigma_{mo}-\left[\sigma_{mo}-2\dfrac{V_f}{V_m}\dfrac{\tau_f}{r_f}\xi-2\dfrac{V_f}{V_m}\dfrac{\tau_i(N)}{r_f}(l_d-\xi)\right]\\ \quad\exp\left(-\rho\dfrac{x-l_d}{r_f}\right), x\in\left(l_d,\dfrac{l_c}{2}\right)\end{cases} \tag{3b}$$